Stochastic fluctuations of the facultative endosymbiont *Wolbachia* due to finite host population size

Jason M. Graham[1], Joseph Klobusicky[1], Michael T.J. Hague[2,*]

[1]Mathematics Department
University of Scranton
Scranton, PA 18510

[2]Biology Department
University of Scranton
Scranton, PA 18510

[*]**Corresponding Author**
Michael T.J. Hague
Biology Department
University of Scranton
800 Linden Street
Scranton, PA 18510
(570) 941-7962
michael.hague@scranton.edu

Keywords: host-microbe interaction, endosymbiosis, maternal transmission, *w*Mel, *Wolbachia*, *Drosophila*

Running Head: Fluctuating *Wolbachia* frequencies

Manuscript Type: Research Article

ABSTRACT

Many insects and other animals host heritable endosymbionts that alter host fitness and reproduction. The prevalence of facultative endosymbionts can fluctuate in host populations across time and geography for reasons that are poorly understood. This is particularly true for maternally transmitted *Wolbachia* bacteria, which infect roughly half of all insect species. For instance, the frequencies of several *w*Mel-like *Wolbachia*, including *w*Mel in host *Drosophila melanogaster*, fluctuate over time in certain host populations, but the specific conditions that generate temporal variation in *Wolbachia* prevalence are unresolved. We implemented a discrete generation model in the new R package *symbiontmodeler* to evaluate how finite-population stochasticity contributes to *Wolbachia* fluctuations over time in simulated host populations under a variety of conditions. Using empirical estimates from natural *Wolbachia-Drosophila* systems, we explored how stochasticity is determined by a broad range of factors, including host population size, maternal transmission rates, and *Wolbachia* effects on host fitness (modeled as fecundity) and reproduction (cytoplasmic incompatibility; CI). While stochasticity generally increases when host fitness benefits and CI are relaxed, we found that a decline in the maternal transmission rate had the strongest relative impact on increasing the size of fluctuations. We infer that non- or weak-CI-causing strains like *w*Mel, which often show evidence of imperfect maternal transmission, tend to generate larger stochastic fluctuations compared to strains that cause strong CI, like *w*Ri in *D. simulans*. Additional factors, such as fluctuating host fitness effects, are required to explain the largest examples of temporal variation in *Wolbachia*. The conditions we simulate here using *symbiontmodeler* serve as a jumping off point for understanding drivers of temporal and spatial variation in the prevalence of *Wolbachia*, the most common endosymbionts found in nature.

INTRODUCTION

Animal life is characterized by diverse interactions with microbes, with relationships spanning a continuum from beneficial to antagonistic. Many insects and other animals carry heritable endosymbionts that are vertically-maternally transmitted from one host generation to the next (Russell et al. 2019; Hague et al. 2024). Endosymbionts can alter basic aspects of host fitness, including reproduction, immune function, and nutrient acquisition (McFall-Ngai et al. 2013; Shropshire et al. 2020; Perreau and Moran 2022; Bennett et al. 2024; Hoffmann and Cooper 2024). The fitness consequences for hosts are ultimately determined by whether or not endosymbionts are prevalent in host populations. Many endosymbionts are facultative from the host perspective, such that a proportion of host individuals in the population do not carry endosymbionts (Mateos et al. 2006; Carrington et al. 2011; Hamm et al. 2014; Corbin et al. 2017; Hague et al. 2020*b*). The frequency of facultative endosymbionts in host populations can vary widely across time, geography, and host systems for reasons that are poorly understood (Hamm et al. 2014; Kriesner et al. 2016; Cooper et al. 2017; Hague et al. 2020*b*; Smith et al. 2021; Wheeler et al. 2021; Gimmi et al. 2023; McPherson et al. 2023).

Maternally transmitted *Wolbachia* are the most common endosymbionts on earth, infecting roughly half of all insect species, as well as other arthropods and nematodes (Ferri et al. 2011; Zug and Hammerstein 2012; Weinert et al. 2015). *Wolbachia* are maternally transmitted through the female germline (Russell et al. 2019; Porter and Sullivan 2023; Radousky et al. 2023; Hague et al. 2024); although, horizontal and introgressive transfers are common on evolutionary timescales (O'Neill et al. 1992; Raychoudhury et al. 2009; Conner et al. 2017; Gerth and Bleidorn 2017; Turelli et al. 2018; Cooper et al. 2019; Vancaester and Blaxter 2023; Shropshire et al. 2024). Patterns of *Wolbachia* spread in nature indicate that the endosymbionts are generally beneficial for host fitness, although these effects are poorly understood in natural populations (Hoffmann and Turelli 1997; Kriesner et al. 2013, 2016; Hamm et al. 2014; Kriesner and Hoffmann 2018; Meany et al. 2019). Recent work suggests *Wolbachia* block viruses in their native *Drosophila* hosts (Hedges et al. 2008; Teixeira et al. 2008; Osborne et al. 2009; Martinez et al. 2014; Cogni et al. 2021; Bruner-Montero and Jiggins 2023), in addition to a potential role of nutrient provisioning (Brownlie et al. 2009; Nikoh et al. 2014; Newton and Rice 2020). Some *Wolbachia* strains also cause cytoplasmic incompatibility (CI), a crossing incompatibility that

generates a frequency dependent benefit that favors *Wolbachia*-positive females (Shropshire et al. 2020; Turelli et al. 2022).

Wolbachia typically occur as facultative endosymbionts in insects (from the host perspective) and are only found in a proportion of host individuals within a given population. *Wolbachia* frequencies can vary considerably in host populations across time and geography for reasons that are poorly understood (Hoffmann et al. 1990; Kriesner et al. 2013, 2016; Hamm et al. 2014; Cooper et al. 2017; Hague et al. 2020*b*, 2022; Wheeler et al. 2021; Turelli et al. 2022). This seems to be particularly true for *Wolbachia* strains that cause no or weak CI. For example, the *w*Mel strain in *D. melanogaster* has been shown to fluctuate dramatically over time at a single locale, with frequency fluctuations >0.7 in some instances and no evidence of seasonality (Hoffmann et al. 1998; Reynolds and Hoffmann 2002). Smaller temporal fluctuations have been observed for the related "*w*Mel-like" *w*San and *w*Yak strains (diverged from *w*Mel ~30,000 years ago) that cause weak CI in *D. yakuba*-clade hosts on the island of São Tomé off the coast of west Africa (Cooper et al. 2017, 2019; Hague et al. 2020*b*). These fluctuating patterns contrast those of strong CI-causing *Wolbachia* strains (e.g., *w*Ri in *D. simulans*), which tend to persist at high, stable frequencies (Hoffmann et al. 1990; Turelli and Hoffmann 1991, 1995; Rousset and Solignac 1995; Bourtzis et al. 1996; James and Ballard 2000; Ballard 2004; Carrington et al. 2011; Choi et al. 2015; Turelli et al. 2018). Examples of temporal frequency variation for strains like *w*Mel suggest that *Wolbachia* may fluctuate stochastically in host populations under certain conditions (Jansen et al. 2008; Kriesner and Hoffmann 2018; Turelli and Barton 2022; Turelli et al. 2022).

We used mathematical models to evaluate how finite-host population stochasticity contributes to *Wolbachia* fluctuations over time in simulated host populations. Population frequencies and equilibria dynamics of *Wolbachia* can be approximated by a discrete generation, deterministic model that incorporates three parameters: (1) the proportion of uninfected ova produced by *Wolbachia*-positive females (μ; i.e., imperfect maternal transmission), (2) the fitness of *Wolbachia*-positive females relative to *Wolbachia*-negative females (F; i.e., components of host fitness like fecundity), and (3) the reduction in the relative egg hatch of uninfected eggs fertilized by *Wolbachia*-positive males due to CI (s_h; i.e., CI strength) (Figure 1) (Hoffmann et al. 1990). Following Turelli et al. (2022) and Turelli and Barton (2022), we adapted the deterministic model of *Wolbachia* equilibria to approximate the stochasticity induced

by finite population size using a stochastic transition matrix analogous to a haploid Wright-Fisher model of genetic drift (Crow and Kimura 1970; Turelli and Barton 2022; Turelli et al. 2022). The model uses an effective population size of N female hosts (because *Wolbachia* are maternally transmitted) and binomial sampling to model the stochastic effects of finite population size in the context of the maternal transmission rate (μ), host fitness effects (F), and the strength of CI (s_h).

We implemented the simulations in a new publicly available R package called *symbiontmodeler*. We used the R package to evaluate how biologically plausible values of host population size ($10^3 \leq N \leq 10^6$), imperfect maternal transmission ($0.001 \leq \mu \leq 0.3$), host fitness effects ($1 \leq F \leq 1.5$), and CI ($s_h = 0, 0.1, 0.45$) influence the size of stochastic *Wolbachia* fluctuations over time in simulated host populations. The package includes additional features to consider a variety of conditions that may occur in natural host populations. For instance, the binomial μ parameter represents imperfect maternal transmission and we allow for inclusion of a subpopulation of "low transmitter" females with especially poor transmission rates, because field estimates of maternal transmission for *w*Mel-like *Wolbachia* suggest that a small proportion of females may have very low transmission (i.e., $\mu > 0.7$) (Hoffmann et al. 1998; Carrington et al. 2011; Hamm et al. 2014; Hague et al. 2020*b*). We also allow for the option of fluctuating host fitness effects by treating F as a log-normal random variable (Turelli et al. 2022), because some evidence suggests that the fitness effects of *w*Mel may be context-dependent (Kriesner et al. 2016; Chrostek et al. 2021). After simulating a wide range of conditions, our results demonstrate how non-CI-causing strains like *w*Mel, which show evidence of imperfect maternal transmission, tend to generate larger stochastic fluctuations over time, as compared to strong-CI-causing strains like *w*Ri.

THEORETICAL FRAMEWORK

Deterministic analysis of Wolbachia frequencies

The deterministic model of *Wolbachia* population frequencies and equilibria dynamics incorporates imperfect maternal transmission (μ), host fitness effects modeled as differential fecundity (F), and CI strength (s_h) (Hoffmann et al. 1990). We assume that uninfected ova produced by *Wolbachia*-positive females (due to imperfect maternal transmission) are susceptible to CI, just as uninfected ova from *Wolbachia*-negative females (Carrington et al.

117 2011). Embryos produced by fertilizations of *Wolbachia*-negative ova with sperm from
118 *Wolbachia*-positive males hatch with frequency $H = 1 - s_h$ relative to the other three possible
119 fertilizations, which are all considered equally compatible (Cooper et al. 2017). Thus, s_h
120 represents the severity of CI, or the reduction in hatch rate due to CI in pairings between
121 *Wolbachia*-negative ova and *Wolbachia*-positive sperm.

122 First, we consider *Wolbachia* strains that do not cause CI ($s_h = 0$), which produce a stable
123 equilibrium ($\hat{p}$) balanced by positive host fitness effects ($F > 1$) and imperfect maternal
124 transmission ($\mu > 0$) (Figure 1). When initially rare, *Wolbachia* must generate $F(1 - \mu) > 1$ to
125 spread deterministically from low frequency, regardless of whether they cause CI. Here, we
126 assume $F(1 - \mu) > 1$ given the spread and persistence of non-CI causing *Wolbachia* strains in
127 nature (Hoffmann and Turelli 1997; Kriesner et al. 2013, 2016; Hamm et al. 2014; Kriesner and
128 Hoffmann 2018; Meany et al. 2019). When $F(1 - \mu) < 1$, rare infections will be deterministically
129 lost (Hoffmann et al. 1990). If $F(1 - \mu) > 1$, the stable equilibrium frequency is

$$\hat{p} = 1 - \frac{\mu F}{F-1}. \quad [1]$$

130 In this case, $\hat{p}$ increases from 0 to $1 - \mu$ as F increases from $1/(1 - \mu)$.

131 Next, we considered equilibria that incorporate CI ($s_h > 0$) (Figure 1). Like non-CI
132 strains, CI-causing strains must still increase host fitness to spread deterministically from low
133 frequency such that $F(1 - \mu) > 1$ (Turelli and Hoffmann 1991, 1995; Bakovic et al. 2018). CI-
134 causing *Wolbachia* that generate $F(1 - \mu) > 1$ and $F\mu < 1$ produce a single stable equilibrium
135 between 0 and 1 given by

$$\hat{p} = \frac{s_h + 1 - F + \sqrt{(s_h + 1 - F)^2 + 4s_h[F(1-\mu) - 1](1 - F\mu)}}{2s_h(1 - F\mu)}. \quad [2]$$

136 Assuming discrete host generations, the total population fraction of offspring in
137 generation $t + 1$ can be divided with respect to whether mated males and females in generation t
138 are carrying *Wolbachia*:

139 1. *Wolbachia-positive male and female*. In this case, there is a population of $F(1-\mu)p_t^2$
140 and also a population of $F\mu(1 - s_h)p_t^2$ when ova become uninfected due to imperfect
141 maternal transmission, resulting in a population fraction of $F(1 - \mu s_h)p_t^2$.

142 2. *Wolbachia-negative male and female*. The population fraction is simply $(1 - p_t)^2$.

143 3. *Wolbachia-negative male, Wolbachia-positive female*. Accounting for fecundity in
144 *Wolbachia*-positive females, the population fraction is then $Fp_t(1 - p_t)$.

4. *Wolbachia-positive male, Wolbachia-negative female*. The population from generation t is $p_t(1-p_t)$. A fraction $1-s_h$ of this population survives from this incompatible pairing, so the population fraction for generation $t+1$ is $p_t(1-p_t)(1-s_h)$.

Assuming equal infection frequencies in males and females, the adult infection frequency in generation t, denoted p_t, changes between generations as follows:

$$p_{t+1} = \frac{p_t F(1-\mu)}{1 + p_t(F-1-s_h) + p_t^2 s_h(1-\mu F)} \quad [3]$$

(Hoffmann et al. 1990). In the absence of CI ($s_h = 0$), this model becomes

$$p_{t+1} = \frac{p_t F(1-\mu)}{1 + p_t(F-1)}. \quad [4]$$

For a stability analysis of [4], see Appendix 1.

Simulations to approximate temporal Wolbachia dynamics under finite population size

Following Turelli and Barton (2022) and Turelli et al. (2022), we approximated the stochasticity produced by finite population size using a stochastic transition matrix analogous to a haploid Wright-Fisher model of genetic drift, which assumes that generations are discrete and the new generation is a random sample of constant population size drawn from the total number of offspring produced by the previous generation (Crow and Kimura 1970). The model uses an effective population size of N females. The finite-population stochasticity, modeled as binomial sampling, is superimposed on the deterministic equilibria dynamics described by [3].

We now derive a model for modeling infection frequency p_t of *Wolbachia*-positive hosts which includes randomness effects from a finite female population of size N, $I_t = Np_t$ of which are infected. We assume females produce the same number of eggs with each mating and that N does not change over generations. Starting with the current adult (female) infection frequency p_t, the infection frequency among viable gametes in the next generation is determined by [3]. Then, the infection frequency in the next generation of N adult females is obtained from binomial sampling of this deterministic projection.

First, we compute the total number of *Wolbachia*-positive adult offspring in generation $t+1$ in the absence of CI ($s_h = 0$). For *Wolbachia*-positive females, we note that there are FI_t ova produced. Each ovum has a probability $1-\mu$ of being infected, so the total number of infected offspring can be represented by a binomial random variable

$$X_t \sim \mathrm{Bin}(FI_t, 1-\mu). \quad [5]$$

For the total number of offspring produced, we observe that all *Wolbachia*-negative females produce *Wolbachia*-negative ova. This gives a total of $N - I$ *Wolbachia*-negative offspring for the next generation. For *Wolbachia*-positive females, we noted that FI_t offspring are produced from matings. This gives a total population of $N + (F-1)I_t$ offspring. The proportion of *Wolbachia*-positive adults for generation $t+1$ is then

$$p_{t+1} = \frac{X_t}{FI_t + N - I_t} = \frac{X_t/N}{p_t(F-1)+1}. \quad [6]$$

From [6], the expected value and variance of p_{t+1}, given knowledge of p_t, are readily computed as

$$\mathbb{E}[p_{t+1}|p_t] = \frac{F(1-\mu)p_t}{p_t(F-1)+1}, \quad \mathrm{Var}(p_{t+1}|p_t) = \frac{F\mu(1-\mu)p_t}{N(p_t(F-1)+1)^2}. \quad [7]$$

From the law of large numbers, as the population $N \to \infty$, the variance in [7] tends to 0, and the random recursion [6] converges to the deterministic model [4]. See Appendix 2 for an analysis of long-term dynamics.

Now, allowing for CI ($s_h > 0$), we can derive a random recursion for p_t. For each of the stages of mating, ova production, and the generation of adult offspring, we record total populations in Table S1. The total *Wolbachia*-positive adult offspring resulting from *Wolbachia*-positive male and female matings is given by $X_1 \sim \mathrm{Bin}(FpI, 1-\mu)$. For *Wolbachia*-negative males and -positive females, total *Wolbachia*-positive offspring is $X_2 \sim \mathrm{Bin}(F(1-p)I, 1-\mu)$. The total number of offspring is found by summing the four terms in the row labeled "adult offspring after CI" in Table S1. Denoting the normalized fractions $\tilde{X}_i = X_i/N$, the fraction of *Wolbachia*-positive offspring over the total population is then

$$p_{t+1} = \frac{\tilde{X}_1 + \tilde{X}_2}{s_h(1-F)p_t^2 + (F - s_h - 1)p_t + s_h\tilde{X}_1 + 1}. \quad [8]$$

As $N \to \infty$, from the law of large numbers [8] approaches the deterministic model [3].

Let us also consider the case where a subpopulation of "low transmitter" *Wolbachia*-positive females with high rates of imperfect maternal transmission are included in the host population. Here, the host population consists of M groups with group fractions $(r_1, \ldots, r_M)$. Rather than a single μ value, the ith subpopulation assumes a value μ_i for $i = 1, \ldots, M$. To compute *Wolbachia*-positive offspring, we are now summing M separate binomial distributions. However, most computations from above carry over. For each group i, we compute $X_i \sim$

$\mathrm{Bin}(FIr_i, 1-\mu_i)$. The number of *Wolbachia*-positive female eggs then becomes $S^M = \sum_{i=1}^{M} X_i$. For no CI, the total population is still $FI + N - I$, and

$$p_{t+1} = \frac{S_{t+1}^M}{FI_t + N - I_t} = \frac{S_{t+1}^M / N}{p_t(F-1)+1}. \quad [9]$$

When $\mu_i \equiv \mu$ for all $i = 1, \ldots, M$, then $S^M \sim \mathrm{Bin}(1-\mu, FI)$ and we recover [6]. Expected values are also straightforward to compute, with

$$\mathbb{E}[p_{t+1}|p_t] = \frac{F(1-\sum_{i=1}^{M} \mu_i r_i)p_t}{p_t(F-1)+1}. \quad [10]$$

Each of the *Wolbachia*-positive populations X_i for $i \ldots, M$ terms are independent, so by additivity of variance,

$$\mathrm{Var}(p_{t+1}|p_t) = \frac{F(\sum_{i=1}^{M} \mu_i(1-\mu_i)r_i)p_t}{N(p_t(F-1)+1)^2}. \quad [11]$$

The stable equilibrium, where $\hat{p} = \mathbb{E}[p_{t+1}|p_t = \hat{p}]$, is very similar to [1]. Accounting for multiple μ_i values, we have

$$\hat{p} = 1 - \frac{F}{F-1} \sum_i \mu_i r_i. \quad [12]$$

Finally, to generalize [8], we replace X_1 and X_2 with sums of independent binomials $\{Y_i\}_{1 \le i \le M}$ and $\{Z_i\}_{1 \le i \le M}$, with

$$X_1 = \sum_{i=1}^{M} Y_i, \qquad Y_i \sim \mathrm{Bin}(Fpr_i I, 1-\mu_i), \quad [13]$$

$$X_2 = \sum_{i=1}^{M} Z_i, \qquad Z_i \sim \mathrm{Bin}(F(1-p)r_i I, 1-\mu_i). \quad [14]$$

We also consider the case where host fitness effects fluctuate from one host generation to the next as independent, identically distributed log-normal random variables (Turelli et al. 2022). Here, we assume that each generation F is chosen independently from a log-normal distribution such that $F = e^X$, where X is a normal random variable with mean μ_X and variance σ^2 (Turelli et al. 2022). This implies that F has median $m = e^{\mu_x}$ and a squared coefficient of variation $CV^2 = \mathrm{Var}(F)/[\mathrm{E}(F)^2] = e^{\sigma^2} - 1$. To produce a particular median, m, and CV for F, we set $\mu_x = \ln(m)$ and $\sigma^2 = \ln(CV^2 + 1)$.

Analysis of biologically plausible parameters values

To explore how μ, F, s_h, and N values influence the size of temporal *Wolbachia* fluctuations, we implemented simulations across a broad range of plausible parameter values informed by empirical estimates for *w*Mel-like *Wolbachia* and field-collected *Drosophila* hosts. For imperfect maternal transmission, we explored a range of μ values based on maternal transmission estimates using field-collected females, as well as females reared under varying conditions in the lab. Estimates of μ ($\pm BC_a$ confidence intervals) for *w*Mel from field-collected *D. melanogaster* range from low (μ = 0.026 [0.008, 0.059]; Hoffmann et al. 1998) up to moderate levels of imperfect transmission (μ = 0.11 [0.07, 0.17]; Olsen et al. 2001). Estimates generated in the lab range as high as μ = 0.415 (0.332, 0.493) when females are reared in the cold (20ºC), as opposed to a standard temperature (25ºC) (Hague et al. 2022, 2024). Estimates of μ for *w*San from field-collected *D. santomea* on São Tomé are moderate (μ = 0.068 [0.027, 0.154]), whereas *w*Yak in *D. yakuba* range from low at low altitude (μ = 0.038 [0.003, 0.184]) to moderate at high altitude (μ = 0.20 [0.087, 0.364]) (Hague et al. 2020*b*). Estimates of μ in the lab for *w*Yak range as high as μ = 0.15 (0.109 0.196) when females are reared in the cold (Hague et al. 2020*b*). Based this information, we explored a broad range of μ values from $0.001 \leq \mu \leq 0.3$.

Previous estimates of μ from a large sample of field-collected female *D. santomea* (N = 62) and *D. yakuba* (N = 71) on São Tomé in 2018 suggest that the majority of females have perfect or near perfect transmission rates, but a small proportion of "low transmitters" have high μ values. For *w*San, the total sample of *Wolbachia*-positive females had a mean value of μ = 0.068 (0.027, 0.154), but 8% of these females had a μ value greater than 0.5 with a mean of μ = 0.728. Similarly, for *w*Yak, the total sample of *Wolbachia*-positive females had a mean value of μ = 0.126 (0.062, 0.238), but approximately 11% of the females had a μ value greater than 0.5 with a mean of μ = 0.803 (Hague et al. 2020*b*). Other work using field-collected females found similar evidence of low transmitters for *w*Mel in *D. melanogaster* (Hoffmann et al. 1998), *w*Suz in *D. suzukii* (Hamm et al. 2014; see Figure 3), *w*Inn in *D. innubila* (Unckless et al. 2009), and *w*Ri in *D. simulans* (Carrington et al. 2011; see Figure 6). Hamm et al. (2014) termed females with high rates of imperfect *w*Suz transmission as "low transmitters" and we follow the same terminology here. Using the *D. yakuba*-clade data as a guide, we explored the effect of including a subpopulation of low transmitters (10% of *Wolbachia*-positive females) with a binomial μ

247 value set to $\mu = 0.8$. Here, the remaining 90% of *Wolbachia*-positive females have μ values set as
248 described above ($0.001 \leq \mu \leq 0.3$).
249 We know far less about *Wolbachia* effects on host fitness in natural populations due to
250 the challenges of estimating F in the wild (Ross et al. 2019*b*). *Wolbachia* cells are found
251 throughout host somatic tissue (Pietri et al. 2016), which is likely to have complex effects on
252 components of host fitness in nature (Hoffmann et al. 1998; Weeks et al. 2007; Kriesner et al.
253 2016; Hague et al. 2020*a*, 2021; Cogni et al. 2021; Bruner-Montero and Jiggins 2023). We
254 generally expect $F > 1$ based of the spread and persistence of *Wolbachia* strains in natural host
255 populations (as described in the model above). Prior experiments found no evidence for
256 fecundity effects of *w*Mel in *D. melanogaster* (Hoffmann et al. 1994) or *Wolbachia* in *D.*
257 *yakuba*-clade hosts (Cooper et al. 2017); however, fecundity represents only one aspect of host
258 fitness. Recent work suggests that *w*Mel blocks viruses in natural populations of *D.*
259 *melanogaster* (Hedges et al. 2008; Teixeira et al. 2008; Cogni et al. 2021; Bruner-Montero and
260 Jiggins 2023). *Wolbachia* effects on other measures of host fitness in the lab have ranged from
261 positive (Brownlie et al. 2009; Russell et al. 2023) to negative (Hoffmann and Turelli 1988;
262 Hoffmann et al. 1990; Kriesner et al. 2016) to context-dependent (Olsen et al. 2001; Fry et al.
263 2004). Beneficial *Wolbachia* effects of $F > \sim 1.2$ (roughly a 20% relative fitness advantage for
264 *Wolbachia*-positive females) have not been documented in any system (Weeks et al. 2007;
265 Hamm et al. 2014; Meany et al. 2019; Hague et al. 2020*b*) and we generally expect values of $F >$
266 1.5 to be biologically unrealistic (Weeks et al. 2007; Hamm et al. 2014; Cooper et al. 2017;
267 Meany et al. 2019; Hague et al. 2020*b*, 2022). Based on this information, we explored how F
268 values ranging from $1 \leq F \leq 1.5$ influence stochastic *Wolbachia* dynamics.
269 It is generally unknown whether host fitness effects fluctuate in natural host populations
270 (Turelli et al. 2022); however, there is evidence that the fitness effects of *w*Mel on *D.*
271 *melanogaster* fecundity (Kriesner et al. 2016) and virus-blocking (Chrostek et al. 2021) can
272 depend on the environmental context. Therefore, we also ran simulations treating F as a log-
273 normal random variable and explored scenarios with weakly ($CV = 0.01$) or strongly ($CV = 0.1$)
274 fluctuating host fitness effects. To illustrate how these values correspond to fluctuating F values
275 in our simulations, when median(F) = 1.05, a $CV = 0.01$ value corresponds to 2.5 and 97.5
276 percentiles of 1.03 and 1.071, respectively, and a $CV = 0.1$ value corresponds to 0.863 and 1.271,
277 respectively.

We investigated three different values of s_h based on estimates of CI strength from field-collected male *Drosophila*. Estimates using *D. melanogaster* males from central and northern Australia suggest that *w*Mel causes weak CI on the order of $s_h = 0.05$ (Hoffmann et al. 1998; Kriesner et al. 2016). CI strength declines rapidly with male age (Shropshire et al. 2021) and Reynolds and Hoffmann (2002) found that one-day-old males derived from wild-collected larvae and pupae produce hatch rates of 0.39 in incompatible crosses, with large confidence intervals (0.15, 0.64). Given this information, Kriesner et al. (2016) conjectured that s_h values of 0 to 0.1 are plausible for *w*Mel, but $s_h > 0.1$ is unlikely. We are not aware of CI estimates for *D. yakuba*-clade *Wolbachia* using field-collected males; however, estimates in the lab indicate these strains reduce egg-to-adult viability in CI crosses by about 10-20% (*w*San: $s_h = 0.15$ [0.12, 0.18]; *w*Yak: $s_h = 0.16$ [0.13, 0.20]; *w*Tei: $s_h = 0.2$ [0.17, 0.23]), although the presence and intensity of CI can vary depending on host and *Wolbachia* genotype (Cooper et al. 2017). Based on these data, we explored the effects of no CI ($s_h = 0$) and weak CI ($s_h = 0.1$) on stochastic *Wolbachia* dynamics. We also considered strong CI ($s_h = 0.45$) characteristic of field-collected male *D. simulans* carrying *w*Ri (Turelli and Hoffmann 1995; Carrington et al. 2011).

For each unique combination of μ, F, and s_h values, we used the *symbiontmodeler* package to run a set of 25 replicate simulations. Each individual simulation began with an arbitrary intermediate *Wolbachia* frequency of $p_0 = 0.4$ and ran for 10,000 host generations (similar p_0 values do not qualitatively alter the results). We removed an initial burn-in of 500 host generations as *Wolbachia* spread from $p_0 = 0.4$ to a stable equilibrium, and then calculated the mean ($\bar{p}$) and standard deviation (p_{SD}) of *Wolbachia* frequencies from generations 501-10,000 for each simulation. We also ran each set of simulations with different plausible values for host population size (N) ranging from 10^3 to 10^6 (McKenzie 1980; McInnis et al. 1982; Powell 1997; Gravot et al. 2004; Bergland et al. 2014). Estimates of local population sizes of *Drosophila* made from mark-release-recapture methods report local census sizes on the order of 10^4 to 10^5 with considerable variation across time and location (McKenzie 1980; McInnis et al. 1982; Powell 1997; Gravot et al. 2004; Bergland et al. 2014).

Finally, to quantify the influence of the different parameter values on temporal *Wolbachia* dynamics, we modeled the $\bar{p}$ and p_{SD} values with linear effects for N, μ, the presence/absence of low transmitters, F, the presence/absence of fluctuating F values (i.e., treating F as fixed or a random variable), and s_h. Because the infection frequency is always

309 between zero and one, we modeled the distribution of the $\bar{p}$ and p_{SD} values as beta random
310 variables. Models were implemented in R version 4.4.2 using the *mgcv* package version 1.9.1
311 (Wood 2017). We found that a small handful of simulations had infections that persisted at $p > 0$
312 for the full 10,000 host generations for combinations of parameter values that do not predict a
313 stable equilibrium of $\hat{p} > 0$ (e.g., $F = 1.05$, $\mu = 0.05$, $s_h = 0$). We removed these simulations from
314 our regression analysis, because they are predicted to be deterministically lost over time and we
315 did not want the $\bar{p}$ and p_{SD} values to bias our analyses of stable equilibria. Finally, we used the
316 "plot_predictions" function from the *marginaleffects* package version 0.25 (Arel-Bundock et al.
317 2024) to visualize the results by generating model predictions for $\bar{p}$ and p_{SD} as a function of the μ
318 value modulated by the presence/absence of low transmitters, F, and s_h.
319
320 **RESULTS AND DISCUSSION**
321 We used *symbiontmodeler* to run a total of 491,400 simulations across 3,276 unique
322 parameter combinations informed by empirical estimates from *Wolbachia-Drosophila* systems
323 and summarized the mean ($\bar{p}$; Figure 2) and standard deviation (p_{SD}; Figure 3) of *Wolbachia*
324 frequencies from each individual simulation. We then used multiple regression to summarize
325 how different values of host population size (N), imperfect maternal transmission (μ), host
326 fitness effects (F), and CI strength (s_h) influence *Wolbachia* frequencies (measured as $\bar{p}$) and the
327 size of stochastic *Wolbachia* fluctuations over time (measured as p_{SD}) in simulated host
328 populations (Figures 4, 5, Tables S2, S3). We first briefly detail how the mean *Wolbachia*
329 frequencies from our stochastic simulations align with equilibria predictions from the strictly
330 deterministic model (Figure 1). Then, we examine the influence of different model parameters on
331 the size of stochastic *Wolbachia* fluctuations, as well as how other factors might contribute to
332 temporal fluctuations in natural host populations.
333 Expectedly, the $\bar{p}$ values from our simulations (Figures 2, 4) closely align with equilibria
334 predictions ($\hat{p}$) from the deterministic model shown in equation [2] (Figure 1), which
335 demonstrates that high rates of maternal transmission (i.e., smaller μ values), strong beneficial
336 host effects, and strong CI yield high equilibrium frequencies. Here, we present simulation
337 results from a population size of $N = 10^4$ as a simple case to illustrate how mean *Wolbachia*
338 frequencies are determined by parameter values of μ, F, and s_h (Figure 6A). Within the range of
339 plausible μ, F, and s_h values we explored, the regression analysis indicated that the value of μ

340 had the strongest relative effect on $\bar{p}$ (β = -22.4, P < 0.001), such that increasing rates of
341 imperfect maternal transmission decrease *Wolbachia* frequencies (Table S2). The value of F had
342 a smaller relative effect than μ on $\bar{p}$ (β = 3.77, P < 0.001), as strong host fitness benefits increase
343 *Wolbachia* frequencies. Finally, the addition of weak CI (s_h = 0.1) had a small effect on $\bar{p}$ (β =
344 0.427, P < 0.001), whereas strong CI characteristic of strains like *w*Ri (s_h = 0.45) had a stronger
345 effect (β = 1.92, P < 0.001) as the frequency dependent benefit of CI drives *Wolbachia* to high
346 frequencies.

347 The inclusion of a subpopulation of low transmitter females (10% of *Wolbachia*-positive
348 females with μ = 0.8) was also associated with lower $\bar{p}$ values (β = -2.43, P < 0.001). We also
349 found an interaction effect between the presence of low transmitters and the μ value (β = 8.26, P
350 < 0.001), such that the rate of decrease in $\bar{p}$ as a function of μ is slightly less when low
351 transmitters are present (Figure 4). While including a subpopulation of low transmitter females
352 generally reduced mean *Wolbachia* frequencies, we note that this effect was strongest for
353 *Wolbachia* strains that do not cause CI (e.g., *w*Mel in *D. melanogaster*). In the $N = 10^4$ example
354 (Figure 6), the no-CI simulations (s_h = 0) without low transmitters had a median $\bar{p}$ value of
355 0.807, which dropped down to 0.472 in the simulations with low transmitters. In contrast, the
356 median $\bar{p}$ value dropped from 0.875 without low transmitters to 0.591 with low transmitters for
357 weak CI (s_h = 0.1) and from 0.945 to 0.858 for strong CI (s_h = 0.45). The impact of low
358 transmitters on $\bar{p}$ is especially strong for relatively small values of μ ($\leq$ 0.01) and F ($\leq$ 1.15),
359 which are otherwise predicted to generate high equilibrium frequencies (Figure 6). For instance,
360 the values of μ = 0.001, F = 1.1, and s_h = 0 generated a pooled mean of $\bar{\bar{p}}$ = 0.989 across 25
361 replicate simulations, but the addition of low transmitters dropped the mean down to $\bar{\bar{p}}$ = 0.11.

362 Studies using field-collected females show that low transmitters are present in some host
363 populations (Hoffmann et al. 1998; Unckless et al. 2009; Carrington et al. 2011; Hamm et al.
364 2014; Hague et al. 2020*b*), but it is generally unclear why heterogeneity in maternal transmission
365 rates exists among individual hosts. Low transmitters could develop if a subpopulation of hosts
366 experience extreme environmental conditions (e.g., a cold bout) that reduce *Wolbachia* densities
367 and perturb maternal transmission (Ulrich et al. 2016; Ross et al. 2017, 2019*a*; Foo et al. 2019;
368 Hague et al. 2020*b*, 2020*a*, 2022, 2024; Chrostek et al. 2021). Thermal conditions can vary on
369 small spatial scales (e.g., individual fruits), so it is plausible that individual females within a
370 population could experience different environmental conditions that impact maternal

371 transmission (Roberts and Feder 2000; Potter et al. 2009; Saudreau et al. 2009; Pincebourde and
372 Woods 2012; Woods et al. 2015). Heterogeneity in *Wolbachia* densities and/or transmission
373 could also arise due to variation in host diet (Serbus et al. 2015; Christensen et al. 2019), age
374 (Reynolds and Hoffmann 2002; Shropshire et al. 2021), and the host and *Wolbachia* genomes
375 (Gu et al. 2022; Hague et al. 2022). For instance, densities of the *w*Inn strain in *D. innubila* host
376 individuals varied by 20,000 fold and correlated with maternal transmission rates in populations
377 sampled in Arizona (Unckless et al. 2009).

378 Next, we used the regression analysis to summarize how different parameter values
379 contribute to the size of stochastic *Wolbachia* fluctuations over time, measured as p_{SD}
380 (Figure 5, Table S3). Again, the value of μ had the strongest relative effect on increasing p_{SD} (β =
381 8.51, $P < 0.001$), such that higher rates of imperfect maternal transmission tend to generate larger
382 *Wolbachia* fluctuations. To a lesser extent, the inclusion of low transmitters also increased p_{SD}
383 values ($\beta = 1.12$, $P < 0.001$). We also found an interaction effect between the value of μ and the
384 presence of low transmitters ($\beta = -4.42$, $P < 0.001$), where the rate of increase in p_{SD} as a
385 function of μ is smaller when low transmitters are present. Beyond maternal transmission rates,
386 the results illustrate an intuitive pattern where strong selection for *Wolbachia* arising from F and
387 s_h is associated with higher *Wolbachia* frequencies ($\bar{p}$) and smaller stochastic fluctuations (p_{SD})
388 (Figure S1). The value of F had a smaller relative effect than μ on p_{SD} ($\beta = -2.04$, $P < 0.001$). If
389 we assume fluctuating host effects and treat F as a log-normal random variable, weak F
390 fluctuations ($CV = 0.01$) only have a minor effect on increasing p_{SD} values ($\beta = 0.423$, $P <$
391 0.001), whereas strong fluctuations predictably have a larger effect ($\beta = 1.78$, $P < 0.001$). The
392 addition of weak CI ($s_h = 0.1$) had a relatively small effect on decreasing p_{SD} values ($\beta = -9.85 \times$
393 10^{-2}, $P < 0.001$). Stronger CI ($s_h = 0.45$) had a larger effect on p_{SD} ($\beta = -0.783$, $P < 0.001$), as
394 strong CI is associated with high, stable infection frequencies. Host population size (N) had only
395 a small relative effect ($\beta = -4.14 \times 10^{-7}$, $P < 0.001$), although p_{SD} predictably declined as
396 population size increased.

397 Broadly, our simulation results are consistent with empirical observations of temporal
398 *Wolbachia* dynamics in natural host populations. *w*Mel-like strains like *w*Mel and *w*San that
399 show evidence of imperfect maternal transmission and cause weak or no CI also tend to fluctuate
400 temporally and spatially in host populations (Hoffmann et al. 1994; Kriesner et al. 2016; Cooper
401 et al. 2017; Hague et al. 2020*b*). For instance, estimates of *w*Mel maternal transmission rates

402 from field-collected female *D. melanogaster* have been recorded as high as μ = 0.11 (0.07, 0.17)
403 and higher values can be generated in the lab by rearing hosts in the cold (Olsen et al. 2001;
404 Hague et al. 2022, 2024). Estimates of CI strength for *w*Mel from field-collected males crossed
405 with *Wolbachia*-negative laboratory females are consistent with $s_h \approx 0$ (unless males are very
406 young) (Hoffmann et al. 1998; Reynolds and Hoffmann 2002; Kriesner et al. 2016; Shropshire et
407 al. 2021). *w*Mel frequencies have been shown to fluctuate significantly over time in host
408 populations in Australia (Hoffmann et al. 1998) and across geography in Australia, North
409 America, and Africa (Kriesner et al. 2016). Similar levels of imperfect maternal transmission
410 have been recorded for *w*San from field-collected *D. santomea* (μ = 0.120, [0.032, 0.346]) and
411 for *w*Yak from *D. yakuba* (μ = 0.20 [0.087, 0.364]) on São Tomé (Hague et al. 2020*b*). *w*San and
412 *w*Yak cause weak CI in the lab (s_h = 0.15 [0.12, 0.18] and s_h = 0.16 [0.13, 0.20], respectively)
413 and their frequencies have both fluctuated temporally on the island of São Tome (Cooper et al.
414 2017; Hague et al. 2020*b*). *w*Yak frequencies also vary by altitude on São Tome (Hague et al.
415 2020*b*). These patterns are by no means characteristic of all *w*Mel-like *Wolbachia*, as some
416 *w*Mel-like strains do cause strong CI in their native hosts (e.g., *w*Seg in *D. seguyi*; Shropshire et
417 al. 2024). Other, more diverged *Wolbachia*, like the *w*Ri-like *w*Suz strain in *D. suzukii* are
418 imperfectly transmitted (μ = 0.14 [0.04, 0.27]), do not cause CI, and persist at intermediate
419 frequencies that vary across time and space (Hamm et al. 2014; Turelli et al. 2018).
420 Notably, across the range of parameter values we explored, declining rates of maternal
421 transmission (i.e., increasing values of μ) had the strongest relative effect on increasing the size
422 of temporal *Wolbachia* fluctuations, as compared to the strength of host fitness effects and CI
423 (Table S3). These results are interesting in light of the fact that maternal transmission rates of the
424 *w*Mel-like strains *w*Mel and *w*Yak are temperature dependent. Both strains exhibit relatively
425 high rates of transmission when hosts are reared in the lab at a standard 25°C (*w*Mel: μ = 0.056
426 [0.022, 0.122], *w*Yak: μ = 0.010 [0, 0.034]), but transmission rates decline when hosts are reared
427 in the cold at 20°C (*w*Mel: μ = 0.197 [0.130, 0.269], *w*Yak: μ = 0.150 [0.106, 0.196]) (Hague et
428 al. 2020*b*, 2024). These results suggest the stochastic fluctuations of *w*Mel-like *Wolbachia* may
429 increase in size under conditions where the maternal transmission rate is perturbed by the
430 environment.
431 The fluctuating patterns of non-CI-causing strains like *w*Mel contrast those of strong-CI-
432 causing *Wolbachia* like *w*Ri in *D. simulans*, which persists at high, stable infection frequencies

433 in nature. *w*Ri generates strong CI ($s_h \approx 0.45$) and seems to have relatively high rates of maternal
434 transmission in the field (e.g., $\mu = 0.026$ [0.004, 0.057]) and perfect transmission in the lab
435 across different temperatures (Hoffmann et al. 1990; Turelli and Hoffmann 1995; Carrington et
436 al. 2011; Kriesner et al. 2013; Hague et al. 2024). Similarly, the CI-causing strains *w*Ha (in *D.*
437 *simulans*) and *w*Ana (in *D. ananassae*) persist at high, stable infection frequencies (Rousset and
438 Solignac 1995; Bourtzis et al. 1996; James and Ballard 2000; Ballard 2004; Choi et al. 2015) and
439 have thermally stable maternal transmission rates in the lab (Hague et al. 2024).
440 Given that some instances of large temporal fluctuations of *w*Mel-like *Wolbachia* have
441 been observed (e.g., >0.7 change in frequency), we also examined the specific combinations of
442 parameters that generate the largest stochastic fluctuations in our simulations. Here, the specific
443 parameters that generated the largest p_{SD} values do not strictly align with the general trends
444 outlined above (Figure 5). Again, we focus on the population size of $N = 10^4$ as a simple case
445 (Figure 6). Assuming strong fluctuating effects on host fitness ($CV = 0.1$), the simulations with a
446 relatively low rate of imperfect maternal transmission ($\mu = 0.01$, no low transmitters), weak host
447 benefits ($F = 1.025$), and no CI ($s_h = 0$) generated the highest average p_{SD} value of $\overline{p_{\mathrm{SD}}} = 0.144$
448 across 25 replicate simulations ($\bar{\bar{p}} = 0.540$) (Figure S2). In this region of parameter space, no CI
449 and the presence of strongly fluctuating F values with a median slightly >1 cause *Wolbachia* to
450 fluctuate between strongly favored ($F[1 - \mu] > 1$) and disfavored ($F[1 - \mu] < 1$) in the host
451 population (Figure S2). A median of value of $F = 1.025$ with $CV = 0.1$ generates 2.5 and 97.5
452 percentiles of 0.843 and 1.251, respectively. These results highlight how a unique set of
453 conditions—particularly fluctuating host effects with a median F value near one—are required to
454 generate the largest stochastic fluctuations in our model.
455 Do host fitness effects fluctuate in natural host populations? Little is known about
456 *Wolbachia* effects on host fitness in nature, although the endosymbionts are generally considered
457 to be beneficial based on the spread and persistence of *Wolbachia* in natural host populations
458 (Weeks et al. 2007; Hamm et al. 2014; Cooper et al. 2017; Meany et al. 2019; Ross et al. 2019*b*;
459 Hague et al. 2020*b*, 2022; Hoffmann and Cooper 2024). While we do not know if host fitness
460 effects fluctuate (Turelli et al. 2022), there is evidence that the effects of *w*Mel on *D.*
461 *melanogaster* fecundity (Kriesner et al. 2016) and virus-blocking (Chrostek et al. 2021) can
462 depend on the environmental context. The non-CI-causing strain *w*Au in *D. simulans* has also
463 been shown to have context-dependent host effects depending on where host breeding occurs

(Cao et al. 2019). Given that temperature has pervasive effects on *Wolbachia* densities in host tissues (Hague et al. 2020*a*, 2024), it is also plausible that temperature-induced changes to *Wolbachia* densities could in turn alter *Wolbachia* effects on various host fitness components.

Our results here serve as a baseline for understanding the contribution of finite-population stochasticity to temporal *Wolbachia* dynamics for *w*Mel-like *Wolbachia*. The dynamics we modeled here may provide a plausible explanation for examples of minor frequency fluctuations, such as temporal variation of *w*Mel in temperate Australia in 1993-96 (Figure S3) (Hoffmann et al. 1998) or fine-scale geographic variation of *w*Yak on the island of São Tomé in 2018 (Figure S4) (Hague et al. 2020*b*). However, the additional assumption of fluctuating host fitness effects is required to explain examples of larger temporal fluctuations (e.g., >0.4 change in frequency), such as *w*Mel variation in subtropical Australia in 1995-96 (Figure S5) (Hoffmann et al. 1998) or *w*San variation on São Tomé in 2005-18 (Figure S5) (Hague et al. 2020*b*).

It is likely that other factors contribute to temporal fluctuations of *w*Mel-like *Wolbachia*, especially given that large fluctuations (e.g., >0.6 change in frequency) have been observed over sampling periods as short as a month (e.g., Figure S5) (Hoffmann et al. 1998). What else could cause *w*Mel-like *Wolbachia* frequencies to fluctuate over time? Perturbation of the maternal transmission rate, for example, due to a change in environmental conditions over time, could cause the equilibrium frequency to decline (Hague et al. 2020*b*, 2022, 2024). In a similar fashion, temporal changes to the strength of host fitness effects or CI could alter *Wolbachia* equilibria, as these parameter can also very depending on environmental conditions, host age, and/or the *Wolbachia* and host genomes (Hoffmann et al. 1990; Clancy and Hoffmann 1998; Olsen et al. 2001; Reynolds and Hoffmann 2002; Bordenstein and Bordenstein 2011; Versace et al. 2014; Kriesner et al. 2016; Cooper et al. 2017; Cao et al. 2019; Shropshire et al. 2021). The model also assumes that hosts have discrete generations and a single, fixed population size. Aspects of insect population dynamics and ecology, such as seasonal variation in population size, could contribute to fluctuating *Wolbachia* frequencies over time (Rasgon and Scott 2004; Farkas and Hinow 2010; Turelli 2010; Hancock et al. 2011; Turelli and Barton 2022). Host migration among structured populations with different *Wolbachia* equilibria dynamics could also plausibly alter frequencies within a given focal population (Hoffmann et al. 1998; Flor et al. 2007; Jansen et al. 2008; Engelstädter and Telschow 2009; Haygood and Turelli 2009; Hancock et al. 2011).

In summmary, our simulations provide a baseline for understanding the stochasticity of temporal *Wolbachia* dynamics, highlighting how non-CI-causing *w*Mel-like strains with relatively poor maternal transmission rates are more likely to fluctuate over time than strong CI-causing strains like *w*Ri. These results motivate further work to explore the incidence and causes of endosymbiont frequency fluctuations in natural host populations. The temporal dynamics of *w*Mel are quite variable at certain locations, but on a broader geographic scale, *w*Mel frequencies persist along a stable latitudinal cline in eastern Australia, raising further questions about the temporal and geographic scales at which *Wolbachia* frequencies vary (Hoffmann et al. 1994, 1998; Kriesner et al. 2016). Studies of *Wolbachia* dynamics within individual host populations on a fine temporal or geographic scale are still relatively uncommon (Turelli and Hoffmann 1995; Hoffmann et al. 1998; Hamm et al. 2014; Kriesner et al. 2016; Cooper et al. 2017; Hague et al. 2020*b*; Wheeler et al. 2021). Moving forward, the publicly available R package *symbiontmodeler* can be used to model how field estimates of maternal transmission, fecundity, and CI at different timepoints or locations contribute to variation in the prevalence of *Wolbachia*, as well as other symbionts (e.g., *Cardinium*; Perlman et al. 2008; Harris et al. 2010). Uncovering sources of temporal and spatial variation in *Wolbachia* prevalence is ultimately critical for predicting endosymbiont spread and the long-term evolutionary dynamics of endosymbiotic relationships.

DATA ACCESSIBILITY STATEMENT

The *symbiontmodeler* R package and scripts to reproduce the regression analysis and figures will be made publicly available upon publication.

COMPETING INTERESTS STATEMENT

The authors declare no competing interests.

AUTHOR CONTRIBUTIONS

JMG: funding acquisition (equal), methodology (equal), formal analysis (lead), software (lead), visualization (lead), writing – original draft (supporting), writing – review and editing (supporting). JK: methodology (equal), formal analysis (supporting), writing – original draft (supporting), writing – review and editing (supporting). MTJH: funding acquisition (equal),

conceptualization (lead), supervision (lead), writing – original draft (lead), writing – review and editing (lead).

ACKNOWLEDGEMENTS

This work was supported by the University of Scranton through a Faculty Internal Research Award to JMG and MTJH and a startup package awarded to MTJH from the College of Arts and Sciences Dean's Office.

535 **FIGURES**

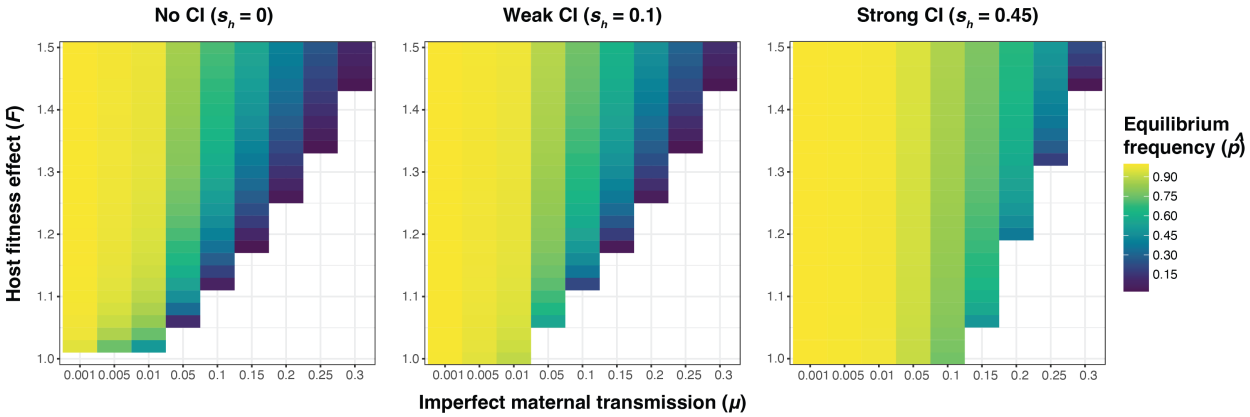

536

537 **Figure 1**. Equilibrium *Wolbachia* frequencies ($\hat{p}$) approximated by a discrete generation
538 deterministic model incorporating imperfect maternal transmission (μ), *Wolbachia* effects on
539 host fitness (F), and cytoplasmic incompatibility (s_h). Equilibrium frequencies are shown across
540 a range of biologically plausible parameter values for no, weak, and strong CI.

541

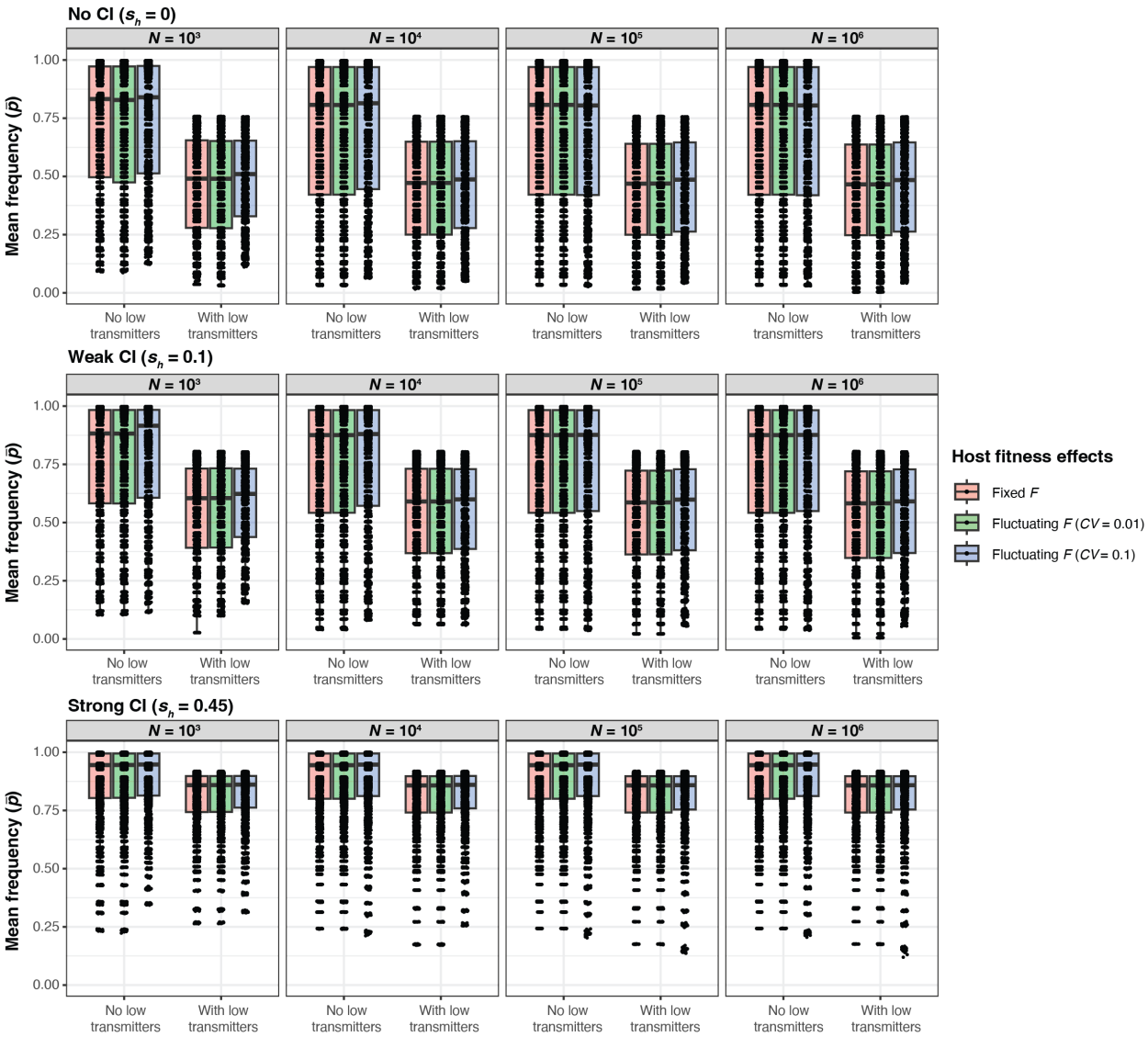

Figure 2. Results from individual simulations exploring the contributions of N, μ, F, and s_h to mean *Wolbachia* frequencies ($\bar{p}$). Each boxplot represents the distribution of $\bar{p}$ values from simulations implemented with different combinations of μ ($0.001 \leq \mu \leq 0.3$) and F ($1 \leq F \leq 1.5$). Datasets are further separated based on whether low transmitters and fluctuating host effects (CV = 0.01 or 0.1) are present. Results are shown for different CI strengths (none, weak, or strong) and population sizes (10^3, 10^4, 10^5, 10^6). Each point represents a $\bar{p}$ value from an individual simulation. The first 500 generations were removed from each simulation before calculating $\bar{p}$.

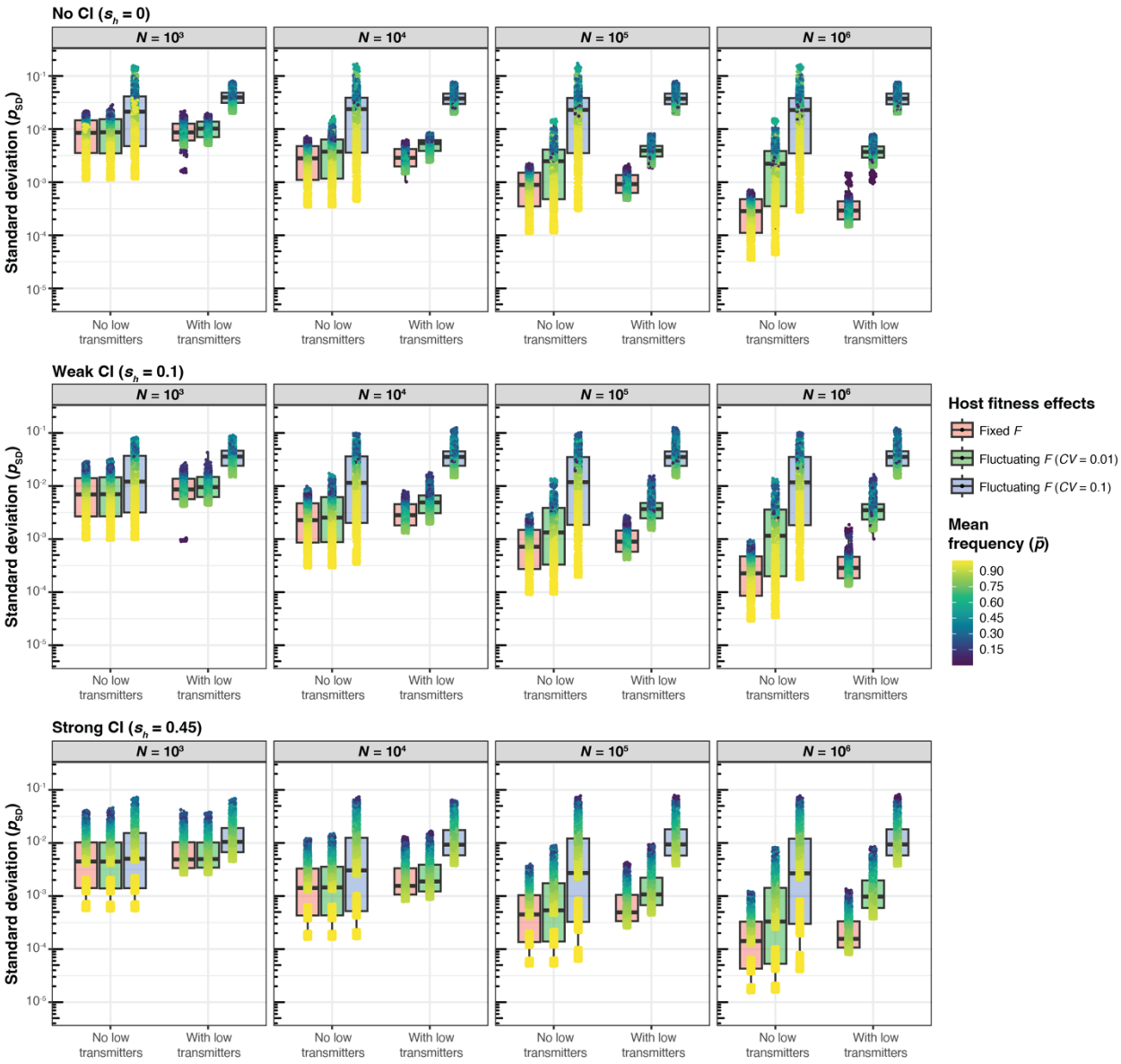

Figure 3. Results from individual simulations exploring the contributions of N, μ, F, and s_h to the standard deviation of *Wolbachia* frequencies (p_{SD}). Each boxplot represents the distribution of p_{SD} values from simulations implemented with different combinations of μ ($0.001 \leq \mu \leq 0.3$) and F ($1 \leq F \leq 1.5$). Datasets are further separated based on whether low transmitters and fluctuating host effects ($CV = 0.01$ or 0.1) are present. Results are shown for different CI strengths (none, weak, or strong) and population sizes (10^3, 10^4, 10^5, 10^6). Each point represents a p_{SD} value from an individual simulation and is color-coded to indicate mean *Wolbachia* frequency ($\bar{p}$) from the simulation. The first 500 generations were removed from each simulation before calculating p_{SD}.

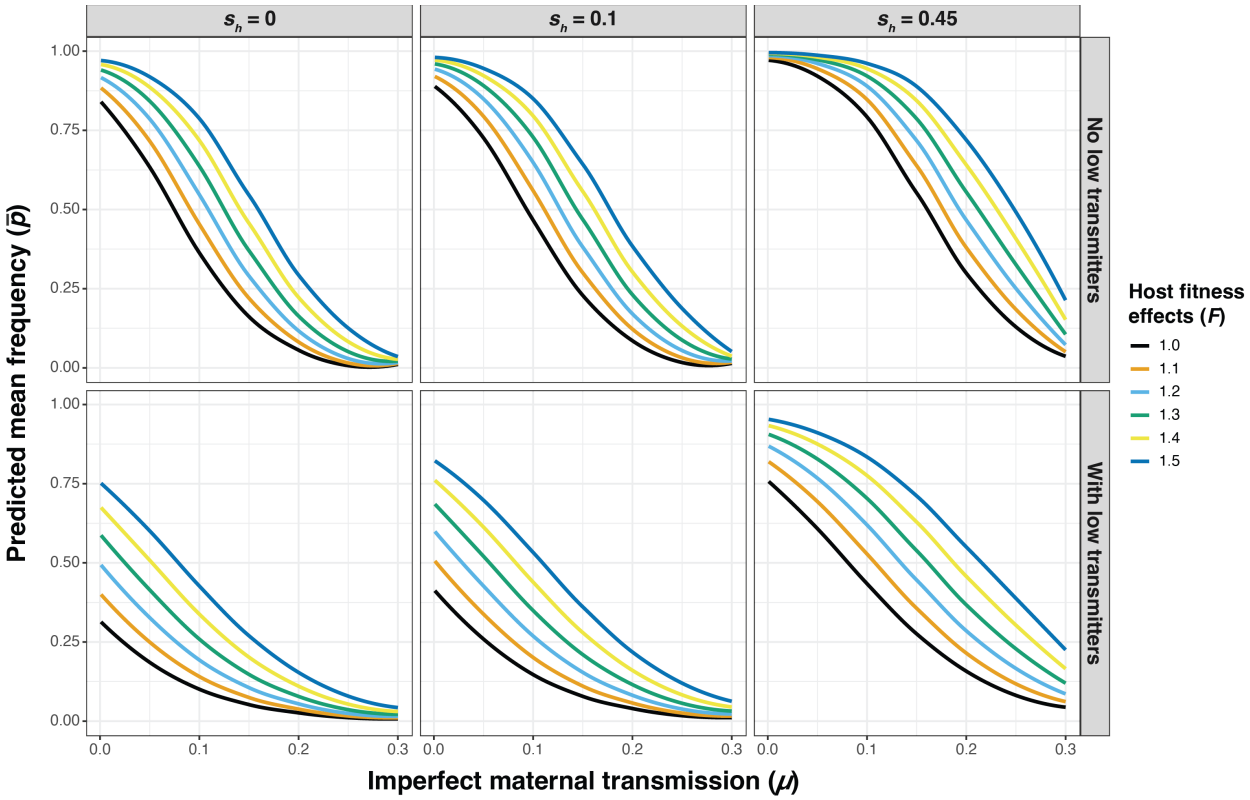

Figure 4. Predicted mean *Wolbachia* frequency ($\bar{p}$) values from the regression analysis as a function of imperfect maternal transmission (μ) and conditioned by the presence/absence of low transmitters, strength of host fitness effects (F), and cytoplasmic incompatibility (s_h). Note that prediction lines average the effects of host population size (N) and fixed/fluctuating host effects (CV = 0.01 and 0.1).

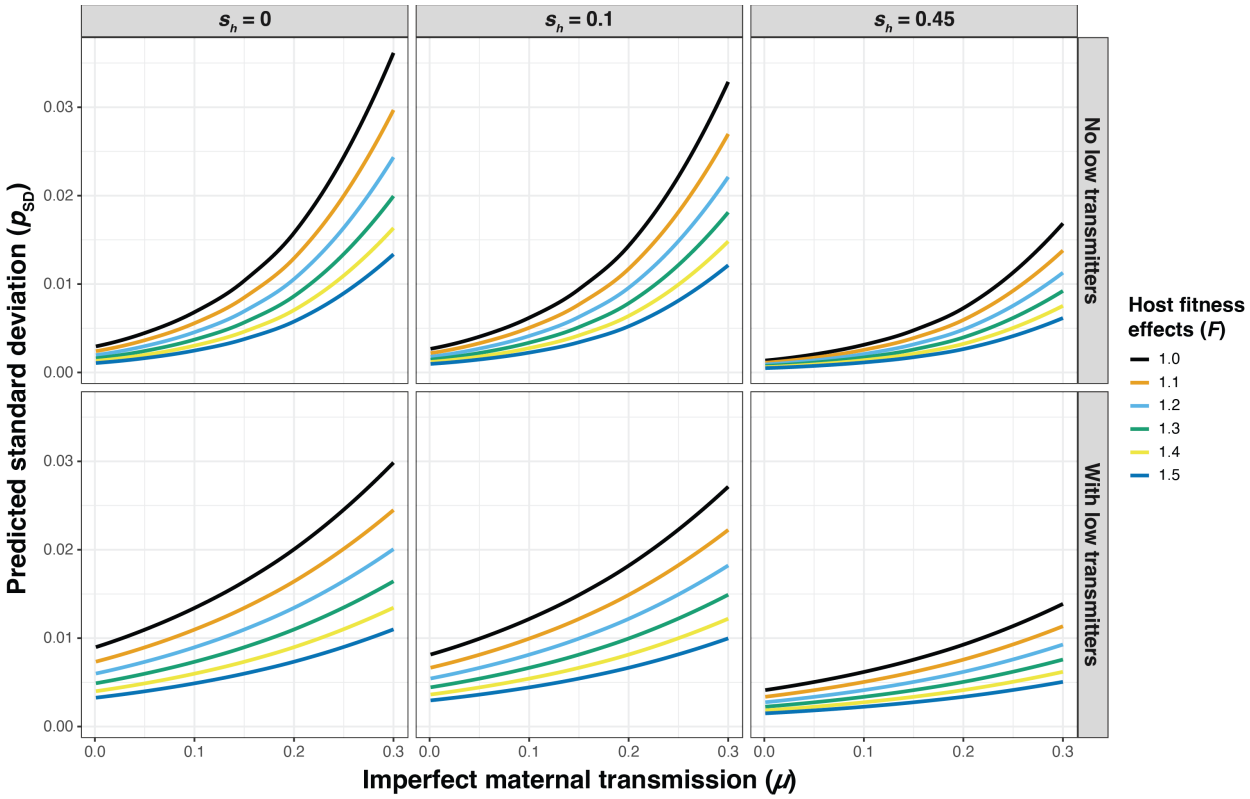

Figure 5. Predicted standard deviation (p_{SD}) values of *Wolbachia* frequencies over time from the regression analysis as a function of imperfect maternal transmission (μ) and conditioned by the presence/absence of low transmitters, strength of host fitness effects (F), and cytoplasmic incompatibility (s_h). Note that prediction lines average the effects of host population size (N) and fixed/fluctuating host effects (CV = 0.01 and 0.1).

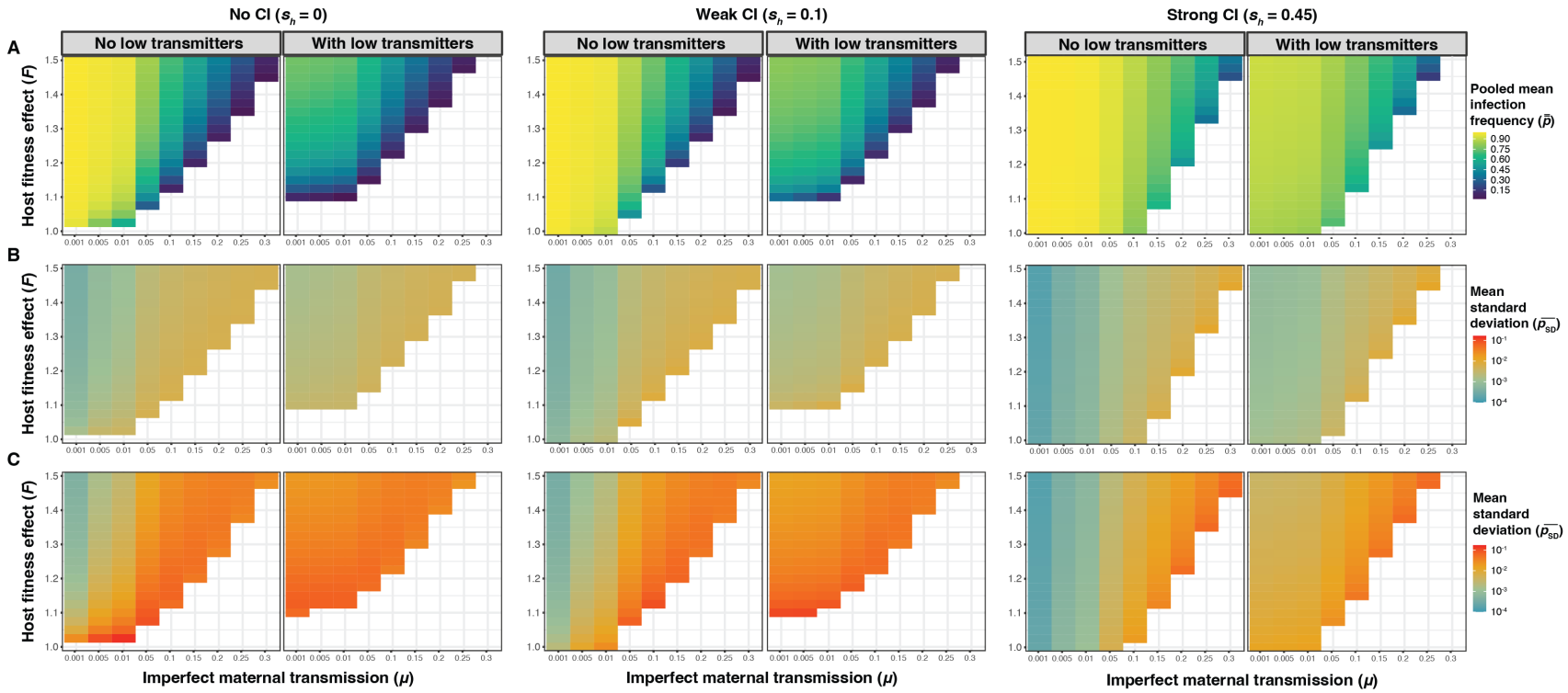

Figure 6. Summary of results from simulations exploring the contributions of μ, F, and s_h to the mean ($\bar{p}$) and standard deviation (p_{SD}) of *Wolbachia* frequencies from simulations with a finite host population size of $N = 10^4$. **(A)** Each cell represents the pooled mean *Wolbachia* frequency ($\bar{\bar{p}}$) from 25 replicate simulations with a set μ and F value. **(B)** Each cell represents the mean standard deviation ($\overline{p_{\mathrm{SD}}}$) of *Wolbachia* frequencies from 25 simulations with a set μ and F value. Note that $\overline{p_{\mathrm{SD}}}$ values are plotted on a log scale. **(B)** Each cell represents $\overline{p_{\mathrm{SD}}}$ from 25 simulations with a set μ and F value with strongly fluctuating fitness effects ($CV = 0.1$). Datasets are further separated based on the presence/absence of low transmitters and CI strength (none, weak, or strong).

579 **LITERATURE CITED**

580 Arel-Bundock, V., N. Greifer, and A. Heiss. 2024. How to Interpret Statistical Models Using
581 marginaleffects for R and Python. Journal of Statistical Software 111:1–32.

582 Bakovic, V., M. Schebeck, A. Telschow, C. Stauffer, and H. Schuler. 2018. Spatial spread of
583 *Wolbachia* in *Rhagoletis cerasi* populations. Biology Letters 14:20180161.

584 Ballard, J. W. O. 2004. Sequential evolution of a symbiont inferred from the host: *Wolbachia*
585 and *Drosophila simulans*. Molecular Biology and Evolution 21:428–442.

586 Bennett, G. M., Y. Kwak, and R. Maynard. 2024. Endosymbioses have shaped the evolution of
587 biological diversity and complexity time and time again. Genome Biology and Evolution
588 evae112.

589 Bergland, A. O., E. L. Behrman, K. R. O'Brien, P. S. Schmidt, and D. A. Petrov. 2014. Genomic
590 evidence of rapid and stable adaptive oscillations over seasonal time scales in *Drosophila*. PLoS
591 Genetics 10:e1004775.

592 Bordenstein, S. R., and S. R. Bordenstein. 2011. Temperature affects the tripartite interactions
593 between bacteriophage WO, *Wolbachia*, and cytoplasmic incompatibility. PLoS One 6.

594 Bourtzis, K., A. Nirgianaki, G. Markakis, and C. Savakis. 1996. *Wolbachia* infection and
595 cytoplasmic incompatibility in *Drosophila* species. Genetics 144:1063–1073.

596 Brownlie, J. C., B. N. Cass, M. Riegler, J. J. Witsenburg, I. Iturbe-Ormaetxe, E. A. McGraw, and
597 S. L. O'Neill. 2009. Evidence for metabolic provisioning by a common invertebrate
598 endosymbiont, *Wolbachia pipientis*, during periods of nutritional stress. PLoS Pathogens
599 5:e1000368.

600 Bruner-Montero, G., and F. M. Jiggins. 2023. *Wolbachia* protects *Drosophila melanogaster*
601 against two naturally occurring and virulent viral pathogens. Scientific Reports 13:8518.

602 Cao, L.-J., W. Jiang, and A. A. Hoffmann. 2019. Life history effects linked to an advantage for
603 *w*Au *Wolbachia* in *Drosophila*. Insects 10:126.

604 Carrington, L. B., J. R. Lipkowitz, A. A. Hoffmann, and M. Turelli. 2011. A re-examination of
605 *Wolbachia*-induced cytoplasmic incompatibility in California *Drosophila simulans*. PLoS One
606 6:e22565.

607 Choi, J. Y., J. E. Bubnell, and C. F. Aquadro. 2015. Population genomics of infectious and
608 integrated *Wolbachia pipientis* genomes in *Drosophila ananassae*. Genome biology and
609 evolution 7:2362–2382.

610 Christensen, S., M. Camacho, Z. Sharmin, A. Z. Momtaz, L. Perez, G. Navarro, J. Triana, et al.
611 2019. Quantitative methods for assessing local and bodywide contributions to *Wolbachia* titer in
612 maternal germline cells of *Drosophila*. BMC Microbiology 19:1–17.

613 Chrostek, E., N. Martins, M. S. Marialva, L. Teixeira, N. A. Moran, and N. Dubilier. 2021.
614 *Wolbachia*-Conferred Antiviral Protection Is Determined by Developmental Temperature. mBio
615 12:e02923-20.

616 Clancy, D. J., and A. A. Hoffmann. 1998. Environmental effects on cytoplasmic incompatibility
617 and bacterial load in *Wolbachia*-infected *Drosophila simulans*. Entomologia Experimentalis et
618 Applicata 86:13–24.

619 Cogni, R., S. D. Ding, A. C. Pimentel, J. P. Day, and F. M. Jiggins. 2021. *Wolbachia* reduces
620 virus infection in a natural population of *Drosophila*. Communications Biology 4:1–7.

621 Conner, W. R., M. L. Blaxter, G. Anfora, L. Ometto, O. Rota-Stabelli, and M. Turelli. 2017.
622 Genome comparisons indicate recent transfer of *w*Ri-like *Wolbachia* between sister species
623 *Drosophila suzukii* and *D. subpulchrella*. Ecology and Evolution 7:9391–9404.

624 Cooper, B. S., P. S. Ginsberg, M. Turelli, and D. R. Matute. 2017. *Wolbachia* in the *Drosophila*
625 *yakuba* complex: Pervasive frequency variation and weak cytoplasmic incompatibility, but no
626 apparent effect on reproductive isolation. Genetics 205:333–351.

627 Cooper, B. S., D. Vanderpool, W. R. Conner, D. R. Matute, and M. Turelli. 2019. *Wolbachia*
628 acquisition by *Drosophila yakuba*-clade hosts and transfer of incompatibility loci between
629 distantly related *Wolbachia*. Genetics 212:1399–1419.

630 Corbin, C., E. R. Heyworth, J. Ferrari, and G. D. Hurst. 2017. Heritable symbionts in a world of
631 varying temperature. Heredity 118:10–20.

632 Crow, J. F., and M. Kimura. 1970. An Introduction to Population Genetics Theory. Harper &
633 Row, New York.

634 Engelstädter, J., and A. Telschow. 2009. Cytoplasmic incompatibility and host population
635 structure. Heredity 103:196–207.

636 Farkas, J. Z., and P. Hinow. 2010. Structured and unstructured continuous models for *Wolbachia*
637 infections. Bulletin of mathematical biology 72:2067–2088.

638 Ferri, E., O. Bain, M. Barbuto, C. Martin, N. Lo, S. Uni, F. Landmann, et al. 2011. New insights
639 into the evolution of *Wolbachia* infections in filarial nematodes inferred from a large range of
640 screened species. PLoS One 6:e20843.

641 Flor, M., P. Hammerstein, and A. Telschow. 2007. *Wolbachia*-induced unidirectional
642 cytoplasmic incompatibility and the stability of infection polymorphism in parapatric host
643 populations. Journal of Evolutionary Biology 20:696–706.

644 Foo, I. J.-H., A. A. Hoffmann, and P. A. Ross. 2019. Cross-generational effects of heat stress on
645 fitness and *Wolbachia* density in *Aedes aegypti* mosquitoes. Tropical Medicine and Infectious
646 Disease 4:13.

647 Fry, A., M. Palmer, and D. Rand. 2004. Variable fitness effects of *Wolbachia* infection in
648 *Drosophila melanogaster*. Heredity 93:379.

649 Gerth, M., and C. Bleidorn. 2017. Comparative genomics provides a timeframe for *Wolbachia*
650 evolution and exposes a recent biotin synthesis operon transfer. Nature Microbiology 2:16241.

651 Gimmi, E., J. Wallisch, and C. Vorburger. 2023. Defensive symbiosis in the wild: Seasonal
652 dynamics of parasitism risk and symbiont-conferred resistance. Molecular Ecology 32:4063–
653 4077.

654 Gravot, E., M. Huet, and M. Veuille. 2004. Effect of breeding structure on population genetic
655 parameters in *Drosophila*. Genetics 166:779–788.

656 Gu, X., P. A. Ross, J. Rodriguez-Andres, K. L. Robinson, Q. Yang, M.-J. Lau, and A. A.
657 Hoffmann. 2022. A *w*Mel *Wolbachia* variant in *Aedes aegypti* from field-collected *Drosophila*

melanogaster with increased phenotypic stability under heat stress. Environmental Microbiology 24:2119–2135.

Hague, M. T., C. N. Caldwell, and B. S. Cooper. 2020*a*. Pervasive effects of *Wolbachia* on host temperature preference. mBio 11:e01768-20.

Hague, M. T. J., J. D. Shropshire, C. N. Caldwell, J. P. Statz, K. A. Stanek, W. R. Conner, and B. S. Cooper. 2022. Temperature effects on cellular host-microbe interactions explain continent-wide endosymbiont prevalence. Current Biology 32:878-888.e8.

Hague, M. T. J., H. A. Woods, and B. S. Cooper. 2021. Pervasive effects of *Wolbachia* on host activity. Biology Letters 17:20210052.

Hague, M. T., H. Mavengere, D. R. Matute, and B. S. Cooper. 2020*b*. Environmental and genetic contributions to imperfect *w*Mel-like *Wolbachia* transmission and frequency variation. Genetics 215:1117–1132.

Hague, M. T., T. B. Wheeler, and B. S. Cooper. 2024. Comparative analysis of *Wolbachia* maternal transmission and localization in host ovaries. Communications Biology 7:727.

Hamm, C. A., D. J. Begun, A. Vo, C. C. Smith, P. Saelao, A. O. Shaver, J. Jaenike, et al. 2014. *Wolbachia* do not live by reproductive manipulation alone: Infection polymorphism in *Drosophila suzukii* and *D. subpulchrella*. Molecular Ecology 23:4871–4885.

Hancock, P. A., S. P. Sinkins, and H. C. J. Godfray. 2011. Population dynamic models of the spread of *Wolbachia*. The American Naturalist 177:323–333.

Harris, L., S. Kelly, M. Hunter, and S. Perlman. 2010. Population dynamics and rapid spread of *Cardinium*, a bacterial endosymbiont causing cytoplasmic incompatibility in *Encarsia pergandiella* (Hymenoptera: Aphelinidae). Heredity 104:239–246.

Haygood, R., and M. Turelli. 2009. Evolution of incompatibility-inducing microbes in subdivided host populations. Evolution 63:432–447.

Hedges, L. M., J. C. Brownlie, S. L. O'Neill, and K. N. Johnson. 2008. *Wolbachia* and virus protection in insects. Science 322:702–702.

Hoffmann, A. A., D. J. Clancy, and E. Merton. 1994. Cytoplasmic incompatibility in Australian populations of *Drosophila melanogaster*. Genetics 136:993–999.

Hoffmann, A. A., and B. S. Cooper. 2024. Describing endosymbiont–host interactions within the parasitism–mutualism continuum. Ecology and Evolution 14:e11705.

Hoffmann, A. A., M. Hercus, and H. Dagher. 1998. Population dynamics of the *Wolbachia* infection causing cytoplasmic incompatibility in *Drosophila melanogaster*. Genetics 148:221–231.

Hoffmann, A. A., and M. Turelli. 1997. Cytoplasmic incompatibility in insects. Pages 42–80 *in* S. L. O'Neill, A. A. Hoffmann, and J. H. Werren, eds. Influential passengers: inherited microorganisms and arthropod reproduction. Oxford University Press.

Hoffmann, A. A., M. Turelli, and L. G. Harshman. 1990. Factors affecting the distribution of cytoplasmic incompatibility in *Drosophila simulans*. Genetics 126:933–948.

Hoffmann, A., and M. Turelli. 1988. Unidirectional incompatibility in *Drosophila simulans*: inheritance, geographic variation and fitness effects. Genetics 119:435–444.

James, A. C., and J. W. O. Ballard. 2000. Expression of cytoplasmic incompatibility in *Drosophila simulans* and its impact on infection frequencies and distribution of *Wolbachia pipientis*. Evolution 54:1661–1672.

Jansen, V. A. A., M. Turelli, and H. C. J. Godfray. 2008. Stochastic spread of *Wolbachia*. Proceedings of the Royal Society of London B: Biological Sciences 275:2769–2776.

Kriesner, P., W. R. Conner, A. R. Weeks, M. Turelli, and A. A. Hoffmann. 2016. Persistence of a *Wolbachia* infection frequency cline in *Drosophila melanogaster* and the possible role of reproductive dormancy. Evolution 70:979–997.

Kriesner, P., and A. A. Hoffmann. 2018. Rapid spread of a *Wolbachia* infection that does not affect host reproduction in *Drosophila simulans* cage populations. Evolution 72:1475–1487.

Kriesner, P., A. A. Hoffmann, S. F. Lee, M. Turelli, and A. R. Weeks. 2013. Rapid sequential spread of two *Wolbachia* variants in *Drosophila simulans*. PLoS Pathogens 9:e1003607.

Martinez, J., B. Longdon, S. Bauer, Y.-S. Chan, W. J. Miller, K. Bourtzis, L. Teixeira, et al. 2014. Symbionts commonly provide broad spectrum resistance to viruses in insects: A comparative analysis of *Wolbachia* strains. PLOS Pathogens 10:e1004369.

Mateos, M., S. J. Castrezana, B. J. Nankivell, A. M. Estes, T. A. Markow, and N. A. Moran. 2006. Heritable endosymbionts of *Drosophila*. Genetics 174:363–376.

McFall-Ngai, M., M. G. Hadfield, T. C. Bosch, H. V. Carey, T. Domazet-Lošo, A. E. Douglas, N. Dubilier, et al. 2013. Animals in a bacterial world, a new imperative for the life sciences. Proceedings of the National Academy of Sciences 110:3229–3236.

McInnis, D., H. Schaffer, and L. Mettler. 1982. Field dispersal and population sizes of native *Drosophila* from North Carolina. The American Naturalist 119:319–330.

McKenzie, J. 1980. An ecological study of the alcohol dehydrogenase (Adh) polymorphism of *Drosophila melanogaster*. Australian Journal of Zoology 28:709–716.

McPherson, A. E., P. K. Abram, C. I. Curtis, E. R. Wannop, J. P. Dudzic, and S. J. Perlman. 2023. Dynamic changes in *Wolbachia* infection over a single generation of *Drosophila suzukii*, across a wide range of resource availability. Ecology and Evolution 13:e10722.

Meany, M. K., W. R. Conner, S. V. Richter, J. A. Bailey, M. Turelli, and B. S. Cooper. 2019. Loss of cytoplasmic incompatibility and minimal fecundity effects explain relatively low *Wolbachia* frequencies in *Drosophila mauritiana*. Evolution 73:1278–1295.

Newton, I. L., and D. W. Rice. 2020. The Jekyll and Hyde symbiont: could *Wolbachia* be a nutritional mutualist? Journal of Bacteriology 202.

Nikoh, N., T. Hosokawa, M. Moriyama, K. Oshima, M. Hattori, and T. Fukatsu. 2014. Evolutionary origin of insect–*Wolbachia* nutritional mutualism. Proceedings of the National Academy of Sciences 111:10257–10262.

Olsen, K., K. T. Reynolds, and A. A. Hoffmann. 2001. A field cage test of the effects of the endosymbiont *Wolbachia* on *Drosophila melanogaster*. Heredity 86:731–737.

O'Neill, S. L., R. Giordano, A. M. Colbert, T. L. Karr, and H. M. Robertson. 1992. 16S rRNA phylogenetic analysis of the bacterial endosymbionts associated with cytoplasmic incompatibility in insects. Proceedings of the National Academy of Sciences 89:2699–2702.

Osborne, S. E., Y. S. Leong, S. L. O'Neill, and K. N. Johnson. 2009. Variation in antiviral protection mediated by different *Wolbachia* strains in *Drosophila simulans*. PLOS Pathogens 5:e1000656.

Perlman, S. J., S. E. Kelly, and M. S. Hunter. 2008. Population biology of cytoplasmic incompatibility: maintenance and spread of *Cardinium* symbionts in a parasitic wasp. Genetics 178:1003–1011.

Perreau, J., and N. A. Moran. 2022. Genetic innovations in animal–microbe symbioses. Nature Reviews Genetics 23:23–39.

Pietri, J. E., H. DeBruhl, and W. Sullivan. 2016. The rich somatic life of *Wolbachia*. MicrobiologyOpen 5:923–936.

Pincebourde, S., and H. A. Woods. 2012. Climate uncertainty on leaf surfaces: the biophysics of leaf microclimates and their consequences for leaf-dwelling organisms. Functional Ecology 26:844–853.

Porter, J., and W. Sullivan. 2023. The cellular lives of *Wolbachia*. Nature Reviews Microbiology 1–17.

Potter, K., G. Davidowitz, and H. A. Woods. 2009. Insect eggs protected from high temperatures by limited homeothermy of plant leaves. Journal of Experimental Biology 212:3448–3454.

Powell, J. R. 1997. Progress and prospects in evolutionary biology: the *Drosophila* model.

Radousky, Y. A., M. T. J. Hague, S. Fowler, E. Paneru, A. Codina, C. Rugamas, G. Hartzog, et al. 2023. Distinct *Wolbachia* localization patterns in oocytes of diverse host species reveal multiple strategies of maternal transmission. Genetics 224.

Rasgon, J. L., and T. W. Scott. 2004. Impact of population age structure on *Wolbachia* transgene driver efficacy: ecologically complex factors and release of genetically modified mosquitoes. Insect Biochemistry and Molecular Biology 34:707–713.

Raychoudhury, R., L. Baldo, D. C. Oliveira, and J. H. Werren. 2009. Modes of acquisition of *Wolbachia*: Horizontal transfer, hybrid introgression, and codivergence in the *Nasonia* species complex. Evolution 63:165–183.

Reynolds, K. T., and A. A. Hoffmann. 2002. Male age, host effects and the weak expression or non-expression of cytoplasmic incompatibility in *Drosophila* strains infected by maternally transmitted *Wolbachia*. Genetics Research 80:79–87.

Roberts, S., and M. Feder. 2000. Changing fitness consequences of hsp70 copy number in transgenic *Drosophila* larvae undergoing natural thermal stress. Functional Ecology 14:353–357.

Ross, P. A., S. A. Ritchie, J. K. Axford, and A. A. Hoffmann. 2019*a*. Loss of cytoplasmic incompatibility in *Wolbachia*-infected *Aedes aegypti* under field conditions. PLoS Neglected Tropical Diseases 13:e0007357.

Ross, P. A., M. Turelli, and A. A. Hoffmann. 2019*b*. Evolutionary ecology of *Wolbachia* releases for disease control. Annual Review of Genetics 53.

Ross, P. A., I. Wiwatanaratanabutr, J. K. Axford, V. L. White, N. M. Endersby-Harshman, and A. A. Hoffmann. 2017. *Wolbachia* infections in *Aedes aegypti* differ markedly in their response to cyclical heat stress. PLOS Pathogens 13:e1006006.

Rousset, F., and M. Solignac. 1995. Evolution of single and double *Wolbachia* symbioses during speciation in the *Drosophila simulans* complex. Proceedings of the National Academy of Sciences 92:6389–6393.

Russell, S. L., J. R. Castillo, and W. T. Sullivan. 2023. *Wolbachia* endosymbionts manipulate the self-renewal and differentiation of germline stem cells to reinforce fertility of their fruit fly host. PLoS Biology 21:e3002335.

Russell, S. L., L. Chappell, and W. Sullivan. 2019. A symbiont's guide to the germline. Current Topics in Developmental Biology 135:315–351.

Saudreau, M., A. Marquier, B. Adam, P. Monney, and H. Sinoquet. 2009. Experimental study of fruit temperature dynamics within apple tree crowns. Agricultural and Forest Meteorology 149:362–372.

Serbus, L. R., P. M. White, J. P. Silva, A. Rabe, L. Teixeira, R. Albertson, and W. Sullivan. 2015. The impact of host diet on *Wolbachia* titer in *Drosophila*. PLoS pathogens 11:e1004777.

Shropshire, J. D., W. R. Conner, D. Vanderpool, A. A. Hoffmann, M. Turelli, and B. S. Cooper. 2024. Rapid host switching of *Wolbachia* and even more rapid turnover of their phages and incompatibility-causing loci. bioRxiv.

Shropshire, J. D., E. Hamant, and B. S. Cooper. 2021. Male age and *Wolbachia* dynamics: investigating how fast and why bacterial densities and cytoplasmic incompatibility strengths vary. mBio 12:e02998-21.

Shropshire, J. D., B. Leigh, and S. R. Bordenstein. 2020. Symbiont-mediated cytoplasmic incompatibility: what have we learned in 50 years? Elife 9:e61989.

Smith, A. H., M. P. O'Connor, B. Deal, C. Kotzer, A. Lee, B. Wagner, J. Joffe, et al. 2021. Does getting defensive get you anywhere?—Seasonal balancing selection, temperature, and parasitoids shape real-world, protective endosymbiont dynamics in the pea aphid. Molecular Ecology 30:2449–2472.

Teixeira, L., Á. Ferreira, and M. Ashburner. 2008. The bacterial symbiont *Wolbachia* induces resistance to RNA viral infections in *Drosophila melanogaster*. PLoS Biology 6:e1000002.

Turelli, M. 2010. Cytoplasmic incompatibility in populations with overlapping generations. Evolution 64:232–241.

Turelli, M., and N. H. Barton. 2022. Why did the *Wolbachia* transinfection cross the road? drift, deterministic dynamics, and disease control. Evolution Letters 6:92–105.

Turelli, M., B. S. Cooper, K. M. Richardson, P. S. Ginsberg, B. Peckenpaugh, C. X. Antelope, K. J. Kim, et al. 2018. Rapid global spread of *w*Ri-like *Wolbachia* across multiple *Drosophila*. Current Biology 28:963-971.e8.

Turelli, M., and A. A. Hoffmann. 1991. Rapid spread of an inherited incompatibility factor in California *Drosophila*. Nature 353:440–442.

Turelli, M., and A. A. Hoffmann. 1995. Cytoplasmic incompatibility in *Drosophila simulans*: dynamics and parameter estimates from natural populations. Genetics 140:1319–1338.

816 Turelli, M., A. Katznelson, and P. S. Ginsberg. 2022. Why *Wolbachia*-induced cytoplasmic
817 incompatibility is so common. Proceedings of the National Academy of Sciences
818 119:e2211637119.

819 Ulrich, J. N., J. C. Beier, G. J. Devine, and L. E. Hugo. 2016. Heat sensitivity of *w*Mel
820 *Wolbachia* during *Aedes aegypti* development. PLoS Neglected Tropical Diseases 10:e0004873.

821 Unckless, R. L., L. M. Boelio, J. K. Herren, and J. Jaenike. 2009. Wolbachia as populations
822 within individual insects: causes and consequences of density variation in natural populations.
823 Proceedings of the Royal Society B: Biological Sciences 276:2805–2811.

824 Vancaester, E., and M. Blaxter. 2023. Phylogenomic analysis of *Wolbachia* genomes from the
825 Darwin Tree of Life biodiversity genomics project. PLoS Biology 21:e3001972.

826 Versace, E., V. Nolte, R. V. Pandey, R. Tobler, and C. Schlötterer. 2014. Experimental evolution
827 reveals habitat-specific fitness dynamics among *Wolbachia* clades in *Drosophila melanogaster*.
828 Molecular Ecology 23:802–814.

829 Weeks, A. R., M. Turelli, W. R. Harcombe, K. T. Reynolds, and A. A. Hoffmann. 2007. From
830 parasite to mutualist: Rapid evolution of *Wolbachia* in natural populations of *Drosophila*. PLoS
831 Biology 5:e114.

832 Weinert, L. A., E. V. Araujo-Jnr, M. Z. Ahmed, and J. J. Welch. 2015. The incidence of bacterial
833 endosymbionts in terrestrial arthropods. Proceedings of the Royal Society B: Biological Sciences
834 282:20150249.

835 Wheeler, T. B., V. Thompson, W. R. Conner, and B. S. Cooper. 2021. *Wolbachia* in the
836 spittlebug *Prosapia ignipectus*: Variable infection frequencies, but no apparent effect on host
837 reproductive isolation. Ecology and Evolution 00:1–12.

838 Wood, S. N. 2017. Generalized additive models: an introduction with R. Chapman and
839 Hall/CRC.

840 Woods, H. A., M. E. Dillon, and S. Pincebourde. 2015. The roles of microclimatic diversity and
841 of behavior in mediating the responses of ectotherms to climate change. Journal of Thermal
842 Biology 54:86–97.

843 Zug, R., and P. Hammerstein. 2012. Still a host of hosts for *Wolbachia*: Analysis of recent data
844 suggests that 40% of terrestrial arthropod species are infected. PLoS One 7:e38544.

845